Atmospheric Environment 137 (2016) 135–145

Contents lists available at ScienceDirect

Atmospheric Environment

journal homepage: www.elsevier.com/locate/atmosenv

Effect of deep injection on field-scale emissions of 1,3-dichloropropene and chloropicrin from bare soil

S.R. Yates [a, *], D.J. Ashworth [b, a], W. Zheng [c], J. Knuteson [d], I.J. van Wesenbeeck [e]

[a] USDA-ARS, U.S. Salinity Laboratory, 450 W. Big Springs Rd., Riverside, CA 92507, USA
[b] University of California, Department of Environmental Sciences, Riverside 92521, USA
[c] Illinois Sustainable Technology Center, University of Illinois at Urbana-Champaign, Champaign, IL 61820, USA
[d] Formerly with Dow Agrosciences, now with FluxExperts, LLC, Indianapolis, IN, USA
[e] Dow Agrosciences, 9330 Zionsville Road, Indianapolis, IN 46268, USA

HIGHLIGHTS

- Fumigant emissions can be reduced by deep injection into soil.
- Mass loss of 1,3-dichloropropene was approximately 15–27%.
- Mass loss of chloropicrin was less than 2% due to high soil reactivity.

ARTICLE INFO

Article history:
Received 5 October 2015
Received in revised form
27 April 2016
Accepted 29 April 2016
Available online 29 April 2016

Keywords:
Soil fumigation
Emissions
1,3-dichloropropene
Chloropicrin
Bare soil
Field experiment
Shank injection
Industrial Source Complex Short Term model (ISCST3)
CALPUFF dispersion model
Aerodynamic gradient method
Integrated horizontal flux method
Theoretical profile shape method

ABSTRACT

Fumigating soil is important for the production of many high-value vegetable, fruit, and tree crops, but fumigants are toxic pesticides with relatively high volatility, which can lead to significant atmospheric emissions. A field experiment was conducted to measure emissions and subsurface diffusion of a mixture of 1,3-dichloropropene (1,3-D) and chloropicrin after shank injection to bare soil at 61 cm depth (i.e., deep injection). Three on-field methods, the aerodynamic (ADM), integrated horizontal flux (IHF), and theoretical profile shape (TPS) methods, were used to obtain fumigant flux density and cumulative emission values. Two air dispersion models (CALPUFF and ISCST3) were also used to back-calculate the flux density using air concentration measurements surrounding the fumigated field. Emissions were continuously measured for 16 days and the daily peak emission rates for the five methods ranged from 13 to 33 μg m^{-2} s^{-1} for 1,3-D and 0.22–3.2 μg m^{-2} s^{-1} for chloropicrin. Total 1,3-D mass lost to the atmosphere was approximately 23–41 kg ha^{-1}, or 15–27% of the applied active ingredient and total mass loss of chloropicrin was <2%. Based on the five methods, deep injection reduced total emissions by approximately 2–24% compared to standard fumigation practices where fumigant injection is at 46 cm depth. Given the relatively wide range in emission-reduction percentages, a fumigant diffusion model was used to predict the percentage reduction in emissions by injecting at 61 cm, which yielded a 21% reduction in emissions. Significant reductions in emissions of 1,3-D and chloropicrin are possible by injecting soil fumigants deeper in soil.

Published by Elsevier Ltd.

1. Introduction

The use of biologically-active organic chemicals (e.g., pesticides, fumigants, etc.) has been essential in the production of an abundant, nutritious and low–cost food supply. Use of synthetic organic chemicals in agricultural production has also resulted in detectable concentrations of pesticides and other compounds of concern in air, soil and water resources.

Agricultural uses of volatile pesticides and soil fumigants may pose a significant threat to human and environmental health if these compounds are transported away from the target zones or persist in soil. Globally, the fumigant methyl bromide (MeBr) was scheduled for phase-out in the year 2005, due to its potential for depleting stratospheric (UNEP, 1992, 1995; Federal Register, 2000). In California, air emission inventories have shown that pesticides

* Corresponding author.
E-mail address: scott.yates@ars.usda.gov (S.R. Yates).

http://dx.doi.org/10.1016/j.atmosenv.2016.04.042
1352-2310/Published by Elsevier Ltd.

and fumigants are significant sources of air pollution. In Fresno County from 1976 to 1995, about 19 tons of pesticide chemicals were emitted into the atmosphere daily (ARB, 1978, 1997a, 1997b), which represents 16% of the reactive organic gas fraction in this region. Unexpectedly high air concentration measurements of an agricultural fumigant 1,3-dichloropropene (1,3-D) prompted a suspension in California between 1990 and 1994 (CDFA, 1990). Soil fumigants may also pose a risk to water supplies due to their generally low soil adsorption properties. For example, movement of 1,3-D to groundwater and fate in aquatic ecosystems have been addressed in several studies (Merriman et al., 1991; Obreza and Onterman, 1991; Yon et al., 1991; Schneider et al., 1995). Bystander exposures to pesticides can be a serious problem related to production agriculture, if not properly managed. With an improved understanding of the mechanisms and processes that affect pesticide transport and fate in soil–water–air systems, it becomes possible to reduce the harmful effects to non-target organisms, and maintain agricultural production, through development of new pesticide management strategies that minimize emissions.

Volatilization and soil degradation are two important routes of fumigant dissipation (Yagi et al., 1995; Majewski et al., 1995; Yates et al., 1996) and several methods have been developed and tested to lower emission losses from soil. These include surface diffusion barriers, such as agricultural films, water seals (Wang et al., 1997,Gao and Trout, 2006), surface soil amendments (Gan et al., 2000; McDonald et al., 2008; Yates et al., 2011), and deep injection (Yates et al., 1997), among others. Deep injection offers a low-cost approach to reduce emissions compared to the use of agricultural films, water seals, soil amendments, or any other approach that requires adding material to a field. With deep injection, emissions can be reduced by decreasing concentration gradients near the soil surface and increasing the soil residence time, which removes chemical fumigants from the soil zone via degradation.

Micrometeorological approaches have been frequently used to measure field-scale pesticide and fumigant emissions from agricultural fields (Glotfelty et al., 1984; Majewski et al., 1995; Yates et al., 1996, 1997; 2015) and include the aerodynamic, integrated horizontal flux, and theoretical profile shape methods. Regulatory approaches have also been used to calculate fumigant emission rates by fitting air dispersion models to measurements of the air concentration collected around a treated field. For example, the California Department of Pesticide Regulations (CDPR) continues to use the Industrial Source Complex Short Term model (ISCST3) (Ross et al., 1996; Barry et al., 1997) for calculating emission rates for regulatory purposes (CDPR, 2008). EPA recently replaced ISCST3 with AERMOD for regulatory use. However, CDPR conducted an analysis and found that the changes incorporated into the AERMOD model did not significantly improve fumigant emission estimates compared to ISCST3. Therefore, CDPR determined that ISCST3 remains appropriate, and their preferred approach, for estimating fumigant emission rates (CDPR, 2008). Other atmospheric dispersion models, such as CALPUFF (Johnson et al., 1999) can also be used to calculate fumigant emission rates.

The soil fumigants 1,3-D and chloropicrin are used to control nematodes and fungi in a variety of vegetable and tree crops. They have relatively high water solubility (~2 g L^{-1}) and short field half-life, and thus, planting can commence within weeks after fumigation. These fumigants also have a relatively high vapor pressure (18–28 mmHg) so that losses to the atmosphere can be significant. In a previous paper, Yates et al. (2015) reported on a field experiment conducted to measure the volatilization rate of 1,3-D and chloropicrin after application to a bare soil at 46 cm depth (SI) using a standard fumigation methodology. Using several methods for quantification, the reported total emissions of 1,3-D and chloropicrin, respectively, ranged from 16 to 35% and 0.3–1.3% of the applied fumigant.

The purpose of the present paper is to obtain emission measurements for soil fumigation employing deep injection, a proposed emission-reduction methodology. By comparison to the standard application methodology reported by Yates et al. (2015) an evaluation can be made to determine if deep injection effectively mitigates emissions.

2. Methods

The deep injection (DI) field experiment was conducted near Buttonwillow, CA in an agricultural field managed by the farmer. The methods for this experiment are the same as Yates et al. (2015) with the exception of injection depth. In brief, the soil is classified as Milham sandy loam (fine-loamy, mixed, thermic Typic Haplargids), with approximately 1% organic matter (upper 10 cm) and decreasing with depth. Two weeks before the experiment the field was disked, plowed and irrigated so that the soil condition was suitable for fumigation (i.e., water content was approximately 0.2 cm^3 cm^{-3} and a friable soil texture). The fumigation rigs had a 450 cm tool bar containing 9 shanks spaced in 50 cm increments laterally. The target depth of application for this field was 61 cm (i.e., 24 inches) and target Telone C-35 application rate was 240 kg/ha (i.e., 20 gal/ac). The field size was 2.8 ha area (178 m by 157 m) and was determined by visually tracking and marking the outside edge of the fumigation rig and tool bar. The total Telone-C35 mass applied to the field was 672 kg and was determined by weighing the tanks before and after fumigation. A chemical analysis of the formulation in the tanks revealed that 430 kg of 1,3-D and 242 kg chloropicrin were applied (see Table 1). After the field was fumigated, nothing further was done to the field and there was no precipitation during the experiment.

2.1. Measurement of 1,3-D and Chloropicrin

XAD-4 (SKC 226-175, SKC, Incorporated, Fullerton, CA) sampling tubes were used to collect 1,3-D and chloropicrin concentrations in the atmosphere at the field site. A charcoal backup tube (SKC 226-09, SKC, Incorporated, Fullerton, CA) was used to check for 1,3-D breakthrough for the field samples. Fumigant measurements were collected at 10, 40, 80, 150, 250 and 400 cm above the ground surface at field center by drawing air through the sampling tubes

Table 1
Application rates and field dimensions.

Experimental treatment	Soil type	Total *cis*-1,3-D applied, kg	Total *trans*-1,3-D applied, kg	Total chloropicrin applied, kg	Field area (ha)	North-South dimension (m)	East-West dimension (m)
Deep injection	Milham sl	215	215	242	2.80	178	157
Standard injection[a]	Milham sl	237	237	222	2.89	162	178

[a] Yates et al. (2015).

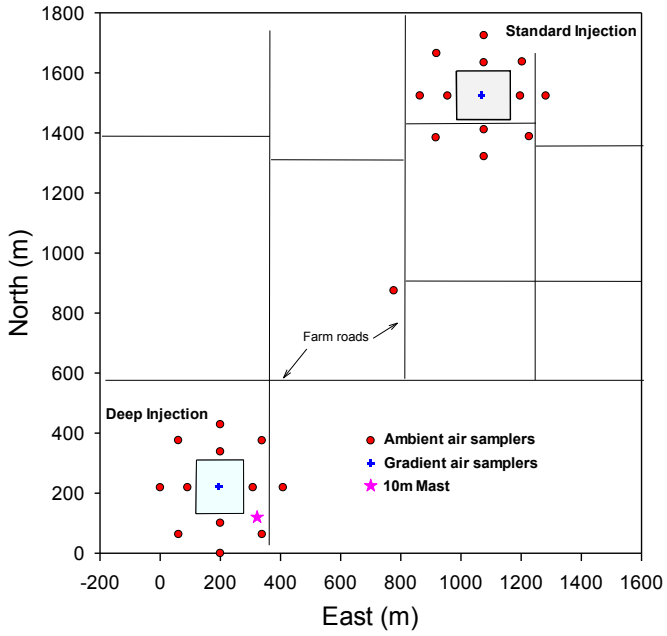

Fig. 1. Site layout and positioning of fields. The experiment conducted at Standard Injection field is described by Yates et al. (2015).

using a vacuum system at a nominal flow rate of 150 cm^3 min^{-1}. Additional samples of the 1,3-D and chloropicrin concentrations in the atmosphere were collected at 1.5 m above the soil surface at 12 locations surrounding the field site (Fig. 1) and had a nominal flow rate of 1.5 L min^{-1}. The sampling tubes were stored in a freezer until chemical analysis.

Chloropicrin and 1,3-D concentrations in the soil gas phase were collected at two locations in the field. The sampling protocol involved the use of stainless steel sampling tubes installed to 5, 10, 25, 50, 75 and 100 cm depths. During sampling, a gas-tight syringe was connected to the stainless steel tube and 50 mL of the soil pore space air phase was drawn through an XAD-4 tube.

2.2. Analysis of 1,3-D and Chloropicrin

Sampling tubes were warmed to room temperature, cut and both sorbent beds were transferred to separate 21-ml head-space vials. Then, 4 mL of n-hexane was added and the vials were immediately sealed with a Teflon-lined septum and aluminum cap. The vials were shaken for 30 min, and then 1 mL of the supernatant was transferred into a 2-mL GC-vial, capped and then stored at −70 °C until GC analysis.

The GC analysis was conducted using an Agilent 6890 series gas chromatograph (Agilent Technologies, Palo Alto, CA) with a micro-electron capture detector (μECD). The column used for the analysis was a 30 m × 0.25 mm DB-VRX column (J & W Scientific, Folsom, CA). The oven, inlet and detector temperatures were 90 °C, 240 °C and 290 °C, respectively. The injection volume was 4.0 μL and the makeup gas was nitrogen with a flow rate of 60 mL/min.

The limits of detection (LOD) and quantification (LOQ) were determined for XAD-4 tubes using this analytical method. For 1,3-D, LOD and LOQ were 0.05 μg/tube and 0.14 μg/tube, respectively. For chloropicrin, LOD and LOQ were 0.004 μg/tube and 0.11 μg/tube, respectively. Further testing revealed that fumigant recovery by XAD-4 at an airflow rate of 0.15 L/min was 86± 5% (1,3-D) and 87± 4% (chloropicrin). An analysis of fumigant recovery from both sorbent beds showed that 98% of the 1,3-D mass and 94% of the chloropicrin mass was found in the front bed. Similar results for chloropicrin were found by Ashworth et al. (2008).

2.3. Meteorological measurements

Wind speed and wind direction (heights 20, 40, 80, 160, 400 cm, Windsonic 2-D, Gill Instruments, Ltd), net radiation (height 100 cm, Q-6, Radiation and Energy Balance Systems, Inc), air temperature (heights 20, 40, 80, 150 cm, fine-wire thermocouples, FW3, Campbell Scientific, Inc.), air temperature and relative humidity (height 150 cm, CS-215, Campbell Scientific, Inc.) and barometric pressure (Vaisala PTA-427, Campbell Scientific, Inc.) were measured at the field center. Solar radiation (LI-200S, LI-COR, Inc.) and 10 m wind speed and wind direction (Wind Monitor, 5305, R.M. Young, Traverse City, MI) were measured near the field (<50 m). Using the 384 hourly-averaged net radiation measurements collected during the experiment, an average and standard deviation was computed for each hour-of-day.

2.4. Methods for measuring the emission rate from soil

Three on-field micrometeorological methods were used to measure the fumigant emission rate from the field: aerodynamic gradient (Parmele et al., 1972), theoretical profiles shape (Wilson et al., 1982), and integrated horizontal flux (Denmead et al., 1977) methods. The aerodynamic gradient method (ADM) utilizes the wind speed, temperature and fumigant concentration gradients to calculate an emission rate (i.e., flux density). The aerodynamic equation for the surface flux, $f_z(0, t)$, is (Rosenberg et al., 1983)

$$f_z(0,t) = \frac{-k^2 z^2}{\varphi_m(t)\varphi_c(t)}\left(\frac{\partial \overline{C}(t)}{\partial z}\right)\left(\frac{\partial \overline{u}(t)}{\partial z}\right)$$

or

$$f_z(0,t) = -k^2\frac{\left[\overline{C}_2(t)-\overline{C}_1(t)\right]\left[\overline{u}_2(t)-\overline{u}_1(t)\right]}{\varphi_m(t)\varphi_c(t)ln(z_2/z_1)^2} = -\Omega_f\frac{\left[\overline{C}_2(t)-\overline{C}_1(t)\right]}{ln(z_2/z_1)} \quad (1)$$

where $f_z(0, t)$ is the interval-averaged vertical flux density at the soil surface [μg m^{-2} s^{-1}], k is von Karman's constant (~0.4), $\overline{u}(t)$ is the averaged wind speed [m s^{-1}], z is height above the soil surface [m] and $\overline{C}$ is the averaged concentration [μg m^{-3}] above the soil surface, φ is a stability correction where the subscripts m and c indicate momentum and fumigant, and Ω_f is the contribution to the flux from meteorological factors.

The ADM method requires a relatively large and spatially–uniform source area and the sampling equipment is usually placed below a maximum height that is approximately 1–2% of the upwind fetch distance, which for this experiments would be between the 80 and 150 cm. Empirical relationships are used adjust the flux for stable and unstable atmospheric conditions (Pruitt et al., 1973).

$$\begin{array}{lll} \varphi_m = (1-16R_i)^{-0.33} & \varphi_c = 0.885(1-22R_i)^{-0.4} & R_i<0 \\ \varphi_m = (1+16R_i)^{0.33} & \varphi_c = 0.885(1+34R_i)^{0.4} & R_i>0 \end{array} \quad (2)$$

where R_i is the Richardson's number $(g/T\,(\partial T/\partial z)\,[\partial u/\partial z]^{-2})$, g is the gravitational acceleration (i.e., 9.8 m s^{-2}), and T is the absolute temperature. Other stability corrections have been proposed in the literature (Brutsaert, 1982; Rosenberg et al., 1983; Fleagle and Businger, 1980). When calculating the emission rates for this experiment, the wind speed and concentration gradients were determined by linear regression (scalar vs natural logarithm of height) using the measurements between the surface and a height of 150 cm.

The theoretical profile shape (TPS) method requires a measurement of wind speed and fumigant concentration at one specific height in the field. The estimate of the volatilization rate is obtained by dividing the product of the wind speed and concentration by a constant correction factor, which is obtained using the trajectory simulation model of Wilson et al. (1982). This method can be used on smaller fields since the height of the sampling equipment is determined *a priori* by conducting an atmospheric simulation of the field for a range of atmospheric conditions and determining a height where the measurements used to obtain the emission rate are minimally affected by atmospheric stability.

The integrated horizontal flux (IHF) method uses a mass balance approach to estimate the emission rate, and requires fumigant concentrations and horizontal wind speeds measurements at several heights above the soil surface (Denmead et al., 1977). This method assumes that emissions are uniformly distributed in the treated area, but does not require corrections for atmospheric stability.

In addition to the on-field flux measurements, two regulatory approaches based on fitting an air dispersion model to air concentration measurements collected around a treated field were also used to calculate the fumigant emission rate. A comprehensive non-steady state Lagrangian puff atmospheric dispersion model, CALPUFF, was used to back calculate the fumigant emission rates for this study (Scire et al., 2000). For computing the flux rate, CALPUFF v6.112 was used with a 2−min time step and an integrated puff sampling approach (i.e. MSLUG = 0). In addition to CALPUFF, the Industrial Source Complex Short Term model (ISCST3), which is currently the preferred approach used by California Department of Pesticide Regulations (CDPR), was used for back-calculating fumigant emission rate (Ross et al., 1996; Barry et al., 1997; CDPR, 2008). Even though Gaussian plume air dispersion models are known to have limitations, which include errors associated with changing meteorology and errors related to near- and far-field distance effects, etc. (Meroney, 1992), CDPR's long history using these approaches for regulatory needs makes their use in calculating fumigant emission rates relevant.

The total mass lost from fumigant emissions (kg) after application to soil, at a particular time, was obtained by summing the product of the period emission rate, sampling period duration, and treated area.

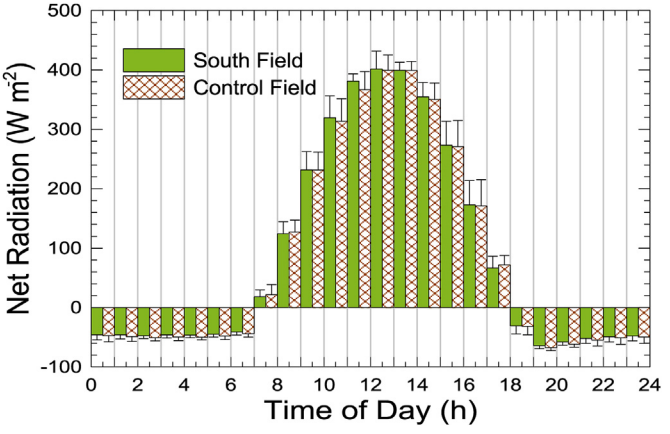

Fig. 2. The net radiation (W m^{-2}) as a function of hour of day at the field site (solid bars). The values are averages over the entire experiment of the hourly net radiation and the error bars are the standard deviations. Crosshatched bars are net radiation measurements simultaneously taken at a nearby field site and reported by Yates et al. (2015). The low standard deviations reflect relatively uniform cloudless conditions throughout the experiment.

3. Results and discussion

Shown in Fig. 1 is the site layout for the deep injection experiment. The treated field was located about 0.85 km southwest of a standard-injection experiment reported by Yates et al. (2015). Fig. 1 shows the layout of the plots and the position of the sampling equipment surrounding each field. An additional air sampler was placed halfway between the two field plots to check for cross contamination. For chloropicrin, all measurements between fields were below the analytical detection limit. For 1,3-D, 14% of the measurements were below the detection limit and the maximum measured concentration between the fields was 7.1 μg m^{-3}, but this value was an order of magnitude lower than near-field concentrations. For the samples above the detection limit, 8%, 58% and 20%, respectively were 4–9, 10–61 and 85–821 times lower than the near-field concentrations.

Soil and environmental conditions at the deep-injection field site were very similar to the standard-injection experiment. For the deep-injection experiment, the air temperature at 0.8 m ranged from 10.2 to 35.5 °C and averaged 22.2 °C. The daily peak temperatures were relatively warm with highs of 30.6 ± 3.6 °C and nighttime lows of 14.2 ± 2.5 °C.

The hourly mean and standard deviation of the net solar radiation (Q_{net}) during the deep-injection experiment (Fig. 2, solid bars), provides a measure of the energy available for soil heating. The Q_{net} data was found to be smoothly varying throughout the day. This indicates relatively continuous clear sky conditions. For comparison purposes, Fig. 2 also shows Q_{net} (crosshatched bars) for the standard-injection experiment conducted simultaneously in a nearby field. In general, the differences between Q_{net} between fields are within one standard deviation during any hourly period. The small standard deviation indicates that soil heating was relatively uniform and predictable by daytime hour. The similarity in Q_{net} between field sites was anticipated due to placement of field sites within the same soil type, and identical field and fumigation management practices. For the deep-injection experiment, the maximum, average, and minimum Q_{net} values, respectively, were 438 W m^{-2}, 88 W m^{-2}, and -72 W m^{-2}. While there are some slight differences in the hour-of-day net radiation measurements between the field sites, the differences all fall well within one standard deviation.

The wind speed at 0.8 m height ranged from 0.31 to 6.95 m s^{-1} and had an average of 1.5 m s^{-1} and the dominant wind direction (i.e., average ± one standard deviation) was 344 ± 66°. In this area of the San Joaquin Valley, the regional wind patterns are affected by the geographic orientation of the valley and surrounding mountains, and leads to winds coming predominately from the NW. The wind rose diagrams (Fig. 3) provide information about the direction of the wind speed, the wind speed velocity and the probability that the wind speed comes from a particular direction. The wind rose diagram reveals that between 14% (10 m height) and 16% (1.6 m height) of the time the winds were from 360 ± 11°. Averaging the high frequency measurements (i.e., 1 min data) collected at 10 m, the resultant average wind direction and wind speed were 331° and 1.37 m s^{-1}, respectively. At 1.6 m, the resultant average wind direction and wind speed were 342° and 1.03 m s^{-1}, respectively. The difference between the average wind direction at 10 m and 1.6 m was likely due to deviations in the orientation of the sensors with respect to North. The diagram also shows that wind speeds in excess of 5 m s^{-1} were observed infrequently, and tended to be from the NW and WNW directions. On an hourly-averaged basis, the maximum wind speeds at 1.6 m were generally below 4 m s^{-1}, with 3.4 ± 1.4 m s^{-1}. The largest value at 1.6 m was 8.0 m s^{-1}, which occurred near the end of the experiment (t = 14.7 d). The largest observed hourly wind speed at height 10 m was 8.8 m s^{-1}. During

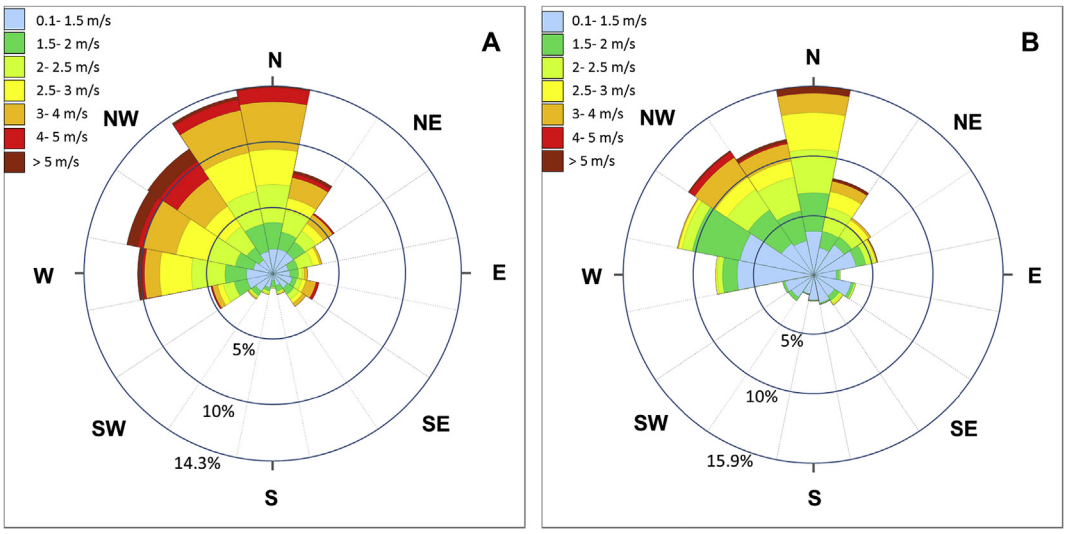

Fig. 3. Wind rose diagrams showing the wind direction, wind speed and frequency that the wind will occur in a specific direction. In A, wind measurements at 10 m are shown. In B, wind measurement at 1.6 m and at field center are shown.

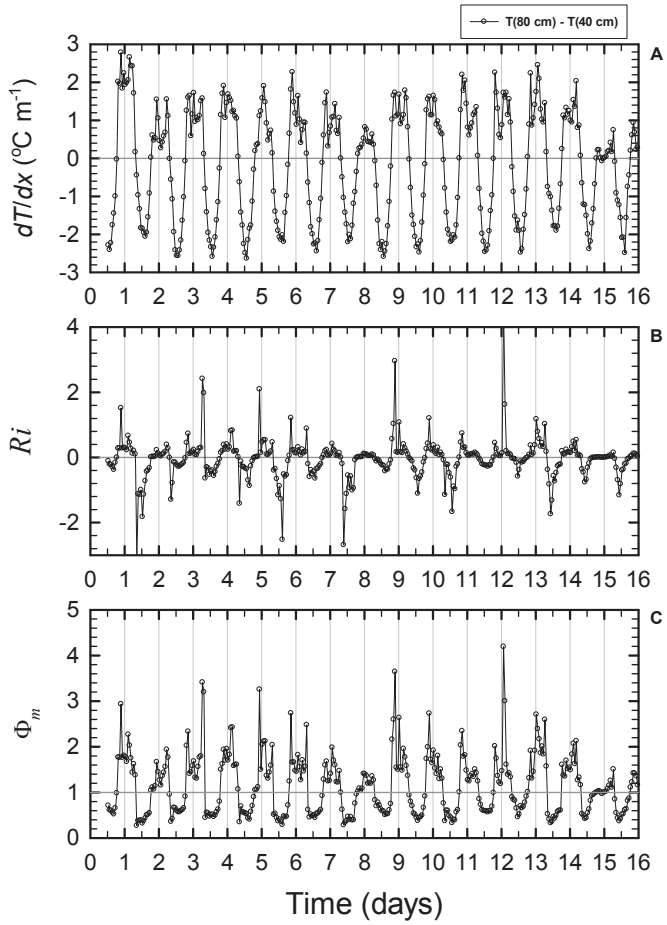

Fig. 4. (A) Temperature difference (A), gradient Richardson's number (B), and atmospheric stability parameter for momentum (C).

nighttime hours, wind speeds were commonly from 0.3 to 0.6 m s^{-1}.

Since two experiments were being conducted simultaneously, the orientation of the fields were based on the highest probability that the observed wind directions (i.e., predominantly from the northwest) would rarely lead to sampling interferences. Over the course of the experiment, the predominant wind direction was indeed from northwest to the southeast (Fig. 3) and rarely were the winds from the NE (i.e., <9% of time) or SW (<3% of time). When this did occur, the NE wind speeds were usually low; less than 2.5 m s^{-1} (6% of time).

The temperature gradient at 60 cm height above the soil surface is shown in Fig. 4A and generally ranged ±3 °C m^{-1} over the experiment. Negative values indicate higher temperatures near the soil surface, which usually occur during unstable conditions (i.e., midday). Near neutral atmospheric conditions occurred consistently near sunrise and sunset each day, and was also observed occasionally at other times. At night, the temperature gradient is positive and is much more erratic compared to daytime values. The gradient Richardson's number (Fig. 4B) and atmospheric stability parameter for momentum (Fig. 4C) were calculated using the temperature and wind speed gradients. The gradient Richardson

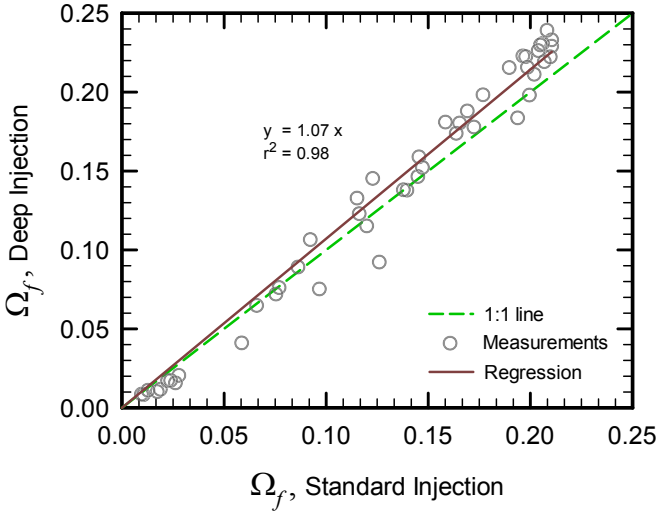

Fig. 5. Comparison of Ω_f (Equation (1)) for standard-injection and deep-injection fields for each sampling period. The slope of the regression line (solid) is close to the 1:1 line (dashed) indicating similar behavior in both fields.

number (*Ri*) is proportional to the temperature gradient, and therefore is zero when the temperature gradient is zero. This provides a means to determine the effect of thermal stability on atmospheric profiles and provides a means to compute the emission rate. During nighttime hours, the momentum stability parameter, Φ_m, was commonly from 2 to 4 with an average and standard deviation of the daily maxima of 2.63 ± 0.76 and during daytime hours the average and standard deviation of the daily minima was 0.37 ± 0.08.

The effect of atmospheric factors on the flux rate can be investigated using Ω_f (Equation (1)). Ω_f provides a means to compare the atmospheric stability differences of the deep-injection and standard-injection fields by eliminating the confounding treatment effects introduced by the concentration gradient. Ω_f provides a method to demonstrate the similarity, or dissimilarity, of the fields and could be used to justify reliance on a single set of wind and temperature measurements in field experiments with nearly identical soil, environmental conditions and field management practices. The relationship shown in Fig. 5 reveals that the soil and micrometeorological behavior of the standard-injection and deep-injection fields were very similar for these experimental fields. The slope of the regression line (solid) was 1.07 (r^2 = 0.98) which is close to the 1:1 line (dashed).

Air concentrations measured in the center of the field, and at surrounding locations 30, 90 and 120 m from the field edge showed expected behavior (Fig. 6). During the first few days, high atmospheric concentrations of 1,3-D were observed at the sampling locations. This is a consequence of the larger chemical concentrations present in the soil shortly after injection, concentration gradients moving fumigant toward the surface, and the rapid fumigant diffusion due to the presence of soil fractures created during fumigation by the shanks. Using a fumigant diffusion model, Yates (2009) showed that shanks produce a more uniform soil concentration and higher concentrations near the soil surface shortly after fumigation, compared to fumigation without a soil fracture. Excavation after fumigation clearly showed the presence of a significant fracture zone (Fig. S1). Air concentrations at later times decreased as the fumigant volatilizes and degrades in soil, which reduce source concentrations and gradients. During the first couple of days, the highest 1,3-D air concentration at 30 m from the field edge was approximately 170 μg m^{-3} and after day 3, a steady reduction in air concentration occurred. At 90 and 120 m from the field edge, the maximum air concentration was from approximately 80 to 110 μg m^{-3}. After approximately day 6, and continuing until the end of the experiment, the daily maximum air concentrations for all distances were an order-of-magnitude less than the earlier daily maxima. Unlike 1,3-D, chloropicrin air concentrations were very low throughout the experiment (data not shown).

Also shown in Fig. 6 is a comparison between 1,3-D concentrations in the atmosphere and two injection depths. For standard injection at 46 cm (Yates et al., 2015), 1,3-D concentrations were generally higher compared to deep injection (i.e., 61 cm) with maxima of approximately 200 μg m^{-3} at 30 m and 120 μg m^{-3} at 90 and 120 m from the field edge. After approximately 3 days, the air concentrations became lower. By 14 days, air concentrations were negligible. The comparison also reveals a similar temporal behavior for standard and deep injection.

3.1. Direct measurement of fumigant emissions

Fumigant emission fractions are used by state and federal regulators to determine various environmental risk endpoints. To reduce bystander exposure and protect public health, an understanding of the transient emission rate is needed. Even infrequent high-level emission events may lead to unacceptable exposure to fumigant vapors. Regulations to reduce near-surface ozone levels also require an understanding of the total atmospheric loading of VOCs to provide an estimate of soil fumigation's contribution to regional VOC.

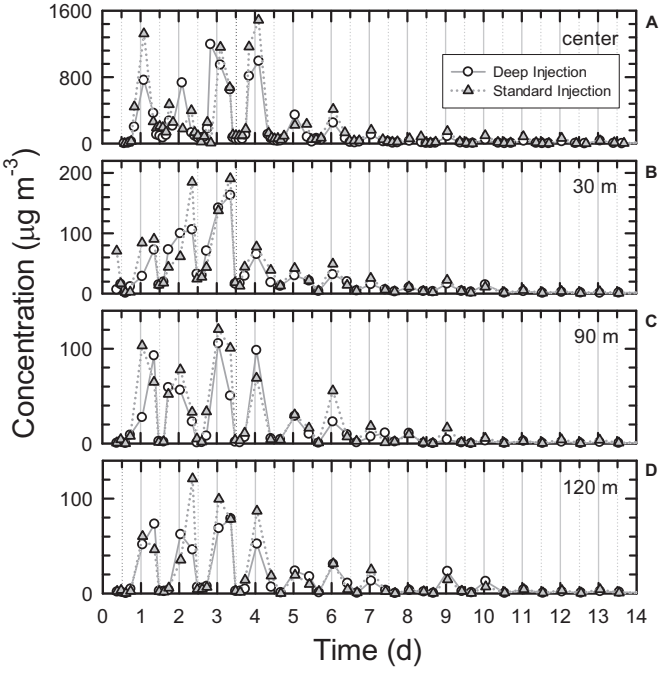

Fig. 6. Comparison of measurements of the 1,3-D concentration at 40 cm height at the center of the field (Center). In Fig. S1 (B–D), concentrations at 1.5 m height are averages of the air monitoring stations surrounding the field site and located at 30 m, 90 m, and 120 m from the edge of the field.

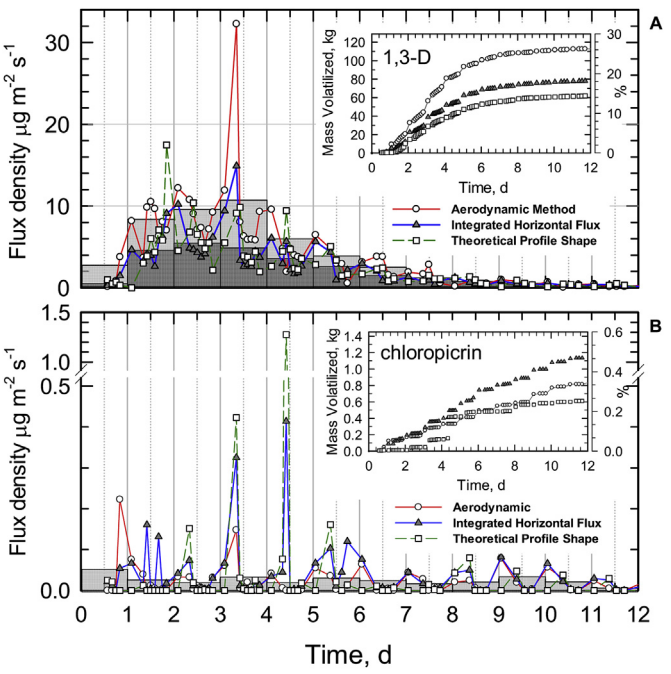

Fig. 7. Volatilization rate (μg m^{-2} s^{-1}) as a function of time (day) after application for the aerodynamic, integrated horizontal flux, and theoretical profile shape methods. Shaded areas are the 24 h average flux values for the ADM (gray) and TPS (stippled) methods. The results are for the DI field.

Table 2
Total emissions of 1,3-D and chloropicrin from the deep-injection plot (DI). The total 1,3-D and chloropicrin mass applied was 430 kg and 242 kg, respectively. For standard-injection plot (SI), the total 1,3-D and chloropicrin mass applied was 474 kg and 222 kg, respectively (Yates et al., 2015).

Fumigant	ADM[a]		IHF[a]	TPS[a]	ISCST3		CALPUFF	
	SI	DI	DI	DI	SI	DI	SI	DI
Total emissions (%)								
1,3-D (cis)	42%	32%	22%	17%	19%	18%	32%	30%
1,3-D (trans)	28%	22%	15%	13%	13%	13%	23%	22%
chloropicrin	1%	0.4%	0.5%	0.3%	1%	0.4%	2%	1%
Telone	35%	27%	19%	15%	16%	16%	28%	26%
Maximum flux rate ($\mu g\ m^{-2}\ s^{-1}$)								
1,3-D (cis)	17.6	18.5	8.6	8.8	7.2	8.2	18.0	19.0
1,3-D (trans)	9.3	13.8	6.3	8.7	4.7	5.3	11.9	14.4
chloropicrin	0.7	0.2	0.4	1.3	0.6	0.6	3.9	3.2
Telone	25.0	32.3	14.9	17.5	11.7	13.2	29.9	33.4

[a] ADM: Aerodynamic method; IHF: Integrated horizontal flux method; TPS: theoretical profile shape method.

Fig. 7 shows time series of the emission rate ($\mu g\ m^{-2}\ s^{-1}$) for the three micrometeorological methods, which include the ADM (circles), IHF (triangles) and the TPS (squares) methods. All the methods exhibit a similar pattern with daily maxima generally coinciding and the peak emission rate (Table 2) for ADM and IHF occurring on day 3 of the experiment, which is followed by very low rates after about 6 days post application. The only exception to this trend was the peak emission rate for TPS occurring on day 1. Throughout the experiment, emission rates calculated from the ADM method tended to be higher than the IHF and TPS methods. In general, the single largest calculated flux, for each method, occurred during the daytime hours at a time of typical atmospheric instability (i.e. morning or evening). But the other daily maxima occurred at various times in response to atmospheric stability conditions in concert with other soil and environmental factors that affect emissions (i.e., concentration gradients in soil, soil drying, etc.).

For 1,3-D, the maximum emission rate of 32.3 $\mu g\ m^{-2}\ s^{-1}$ was obtained with the aerodynamic method, and occurred at 3.35 d. The largest emission rate for the IHF method (14.9 $\mu g\ m^{-2}\ s^{-1}$) also occurred during this time period. The maximum emission rate calculated with the TPS method was 17.5 $\mu g\ m^{-2}\ s^{-1}$ and occurred at 1.84 d and the emission rate at 3.35 d was 9.1 $\mu g\ m^{-2}\ s^{-1}$. Except for the maximum flux rate, the three methods provide similar behavior in the average volatilization rates (see shaded areas), with increasing values to about 3 days then tailing off afterwards.

The cumulative 1,3-D emission as a function of time after application is shown in Fig. 7 (inset). At 12 d, the cumulative emission calculated with the ADM is 27%, and the IHF and TPS were lower at 19 and 15%, respectively (Table 2). The ADM method yielded a cumulative emission that was 42–80% larger than the other methods, and was a result of consistently higher emission rates throughout the experiment. When 1,3-D is applied at a depth of 46 cm (Yates et al., 2015) emissions calculated using the ADM were 35% (Table 2, SI). In previous research that used these methods for calculating the fumigant emission rate, it was found that the ADM was approximately 50% higher than the IHF and TPS methods (Yates et al., 2008). For this study, the trend in total emissions was found to follow ADM > IHF > TPS.

For chloropicrin, emission rates were <1.5 $\mu g\ m^{-2}\ s^{-1}$. The low emission rates were due to high soil degradation rates observed for this soil type (Yates et al., 2015) and low chloropicrin application rates, leading to relatively low soil concentrations (Ashworth et al., 2015). The total chloropicrin emissions were found to be less than 1% of applied for this study and less than 2% when injected at 46 cm (Table 2, SI). This is consistent with the study by Ashworth et al. (2015) which showed that chloropicrin emissions from a mixture of 1,3-D (65%) and chloropicrin (35%) applied at a rate of approximately 157 kg ha^{-1} resulted in <2% emission of chloropicrin. It was also shown that the emission rate of chloropicrin drops dramatically at application rates below 100 kg ha^{-1} even in the presence of significant quantities of 1,3-D. The low atmospheric concentrations measured for chloropicrin increases the uncertainty in the flux estimates, especially for the ADM, which with uses the concentration gradient.

Short-term emission measurements tend to be highly variable during the day. Integrating the short-term emission rates over a 24 h period produces smoothing and shows a more predictable behavior that starts with an increase in the 24-h emission rate after fumigation, reaching a maximum on day 3, and is followed by a long period of decreasing values (see shaded areas in Fig. 7). The 24-h emission rates could be mathematically modeled using conventional transport approaches (Jury et al., 1983; Yates, 2009; Yates et al., 2015).

The dynamics of the emission process changed with time after injection. Investigating the behavior of the average emission rate (Fig. 8), helps to reduce the variability as a function of time, and more clearly reveals the underlying behavior of the volatilization process. Shortly after injection the emission rate increased in response to large fumigant concentration gradients in soil, and the peak emission rates occur near midnight, in an overall increasing pattern. Starting day 2, the emission rates decrease during the early afternoon in response to evaporation reducing the water content of the soil surface. The drying of the soil surface in response to solar energy inputs has been suggested as a cause of reduced emission rate since very dry soil tends to have increased vapor phase adsorption (Spencer et al., 1969; Glotfelty et al., 1984; Reichman et al., 2011, 2013a,b). Vapor adsorption has been shown to strongly bind volatile pesticides to soil particles in a highly nonlinear process (Spencer and Cliath, 1973), which reduces the vapor density in the soil air phase.

3.2. Indirect measurement of fumigant emissions

The emissions of 1,3-D obtained using the ISCST3 and CALPUFF (Fig. 9) back-calculation methods show similar behavior to the micrometeorological methods, with increasing rates early in the experiment and decreasing rates after about 2 days. The peak emission rate for CALPUFF and ISCST3 were 33 and 13 $\mu g\ m^{-2}\ s^{-1}$, respectively. The short-term emission rates using ISCST3 were found to be consistently lower than estimates obtained using the CALPUFF model (approximately 50% lower on average). The largest differences occurred after sunrise and before solar noon, where the ISCST3 emissions could be as much as 90% lower than CALPUFF

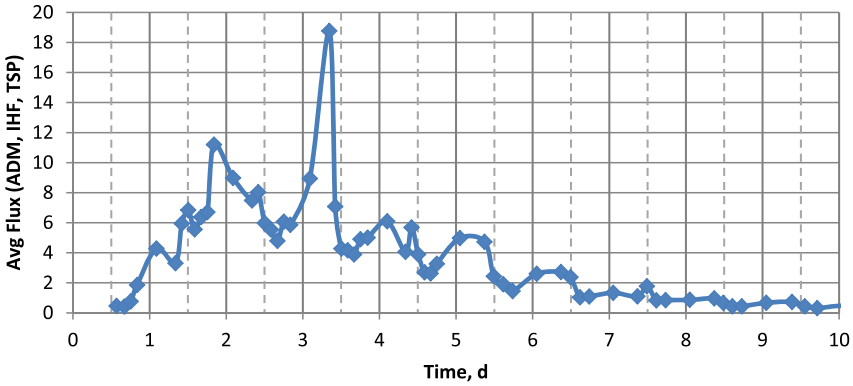

Fig. 8. Average 1,3-D volatilization rate (μg m^{-2} s^{-1}) as a function of time (day) after application for the DI field experiment. Values were calculated by averaging the aerodynamic, integrated horizontal flux, and theoretical profile shape methods at each time point.

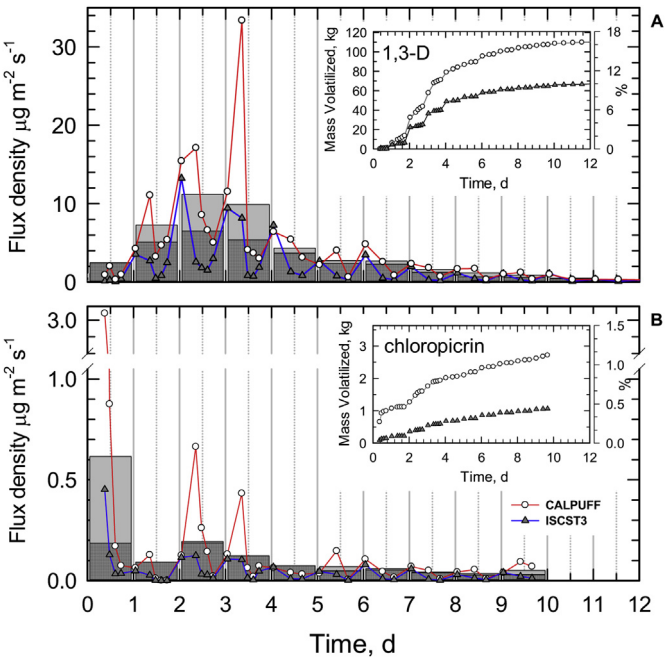

Fig. 9. Volatilization rate (μg m^{-2} s^{-1}) as a function of time (day) after application for the ISCST3 and CALPUFF method. Shaded areas are the 24 h average flux values for the CALPUFF (gray) and ISCST3 (stippled) methods. The results are for the DI field.

values. The reported ISCST3 total 1,3-D volatilization losses were 39% lower than the CALPUFF values. This is similar to the results reported by Yates et al. (2015) who found that the total emission losses from ISCST3 were 40% less than CALPUFF. The 24 h averaged emission rate for 1,3-D revealed a similar pattern as shown in Fig. 9 for the micrometeorological methods with an increasing emission rate after fumigation, and decreasing emission rate after about 3 days.

For chloropicrin, the largest emission rates occurred during the first measurement period with calculated CALPUFF and ISCST3 emission rates of 3 and 0.5 μg m^{-2} s^{-1}, respectively. This was the period when fumigation was occurring and the high emission rates are likely associated with fumigant losses when raising and lowering the shank injectors while turning the injection rig. Compared to the micrometeorological methods, the total emissions were also estimated to be very low, <1.5% of applied. Total emissions from the ISCST3 method were 61% less than CALPUFF, which is similar to Yates et al. (2015) who reported ISCST3 total emissions were 56% less than CALPUFF. The measured emissions of chloropicrin during this study were different from emission rates reported in the literature, which can exceed 30% of the applied fumigant. As discussed by Yates et al. (2015), this was attributed to unusually high soil reactivity at the field site, and was also verified by using a fumigant diffusion model.

3.3. Fumigant concentration in the soil gas phase

Fig. 10 shows the 1,3-D (A) and chloropicrin (B) gas-phase concentration and the soil water content (C) at several depths and times after application. Shown in Fig. S2 is the soil temperature during the experiment. For day 1, the concentration of 1,3-D and chloropicrin in the soil gas phase at 0.5 m depth was approximately 14 and 5.5 μg cm^{-3}, respectively. It is evident that diffusion in soil begins immediately after application and leads to increased concentrations with depth. At later times (e.g., after ~ 6 days), the size of treatment zone increased and had a relatively uniform concentration.

Two field experiments were conducted in 2005 in near-by fields, and with similar experimental conditions. Field experiment 2005A (Yates et al., 2008) studied the effect of surface water seals on 1,3-D emissions and experiment 2005B (Yates et al., 2011) studied the effect of soil organic amendments on 1,3-D emissions. For both experiments, soil gas concentrations were measured at a depth of 0.45 m for several days after fumigation. For 2005A, the measured soil gas concentrations on days 1, 2, 3 and 4, respectively, were 29.0, 11.7, 4.57 and 2.05 μg cm^{-3}. For 2005B, the measured soil gas concentrations on days 1, 2, 3, 4 and 11, respectively were 25.5, 13.0, 6.6, 3.93, and 0.038 μg cm^{-3}. The higher soil gas concentrations during the 2005 experiments was due to the depth of the soil gas samplers, which was 1 cm above the injection depth (0.46 m). For the deep-injection experiment, the distance between the soil gas sampler and the injection depth was 11 cm. To make a comparison with the soil gas concentration measurements from the 2005A and 2005B experiments, a soil fumigant diffusion model (i.e., Yates, 2009) model was used to estimate soil gas concentrations at 0.60 cm, 1 cm above the injection depth. Doing this leads to 1,3-D concentrations of 27, 17, 12, and 9 g cm^{-3}, which are similar to the measured soil gas concentrations 1 cm above the injection depth during the 2005 experiments. The similarities between experiments provide evidence that the observed differences in emission rates are due to treatment effects (i.e., deep injection, water seals, and organic amendments).

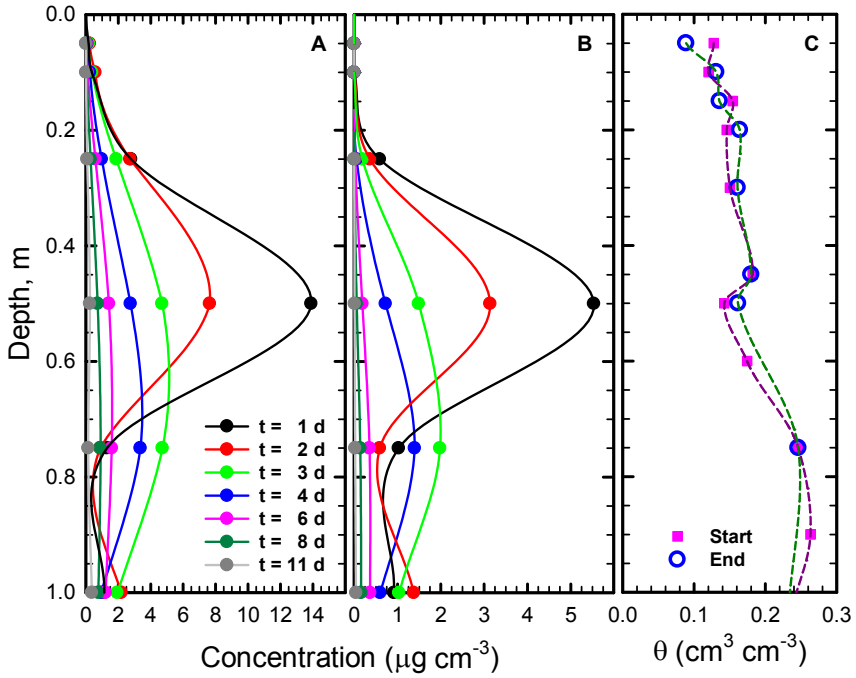

Fig. 10. (A) Telone II (1,3-D cis + trans) soil gas phase concentration (μg cm^{-3}) with depth in soil. (B) Chloropicrin soil gas phase concentration (μg cm^{-3}) with depth in soil. Each line represents the concentration distribution at a particular time after application. In (C), the initial and final soil water content (cm^3 cm^{-3}) with depth are presented. The results are for the DI field.

4. Conclusions

One goal of this research was the comparison of emissions for several emission reduction strategies, including deep injection. The similarities between measurements of soil and environmental conditions across the treatments provide evidence that comparing emission rates and total emissions would be valid. Using the micrometeorological and back-calculation methods to estimate total emissions of 1,3-D and chloropicrin for the experiment, it was found that the methods were in agreement to within approximately 20 ± 6% for 1,3-D and 0.6 ± 0.3% for chloropicrin. The reduction in total 1,3-D emissions by increasing the injection depth from 46 cm (Yates et al., 2015) to 61 cm (deep injection) ranged from 2% (ISCST3) to 24% (ADM) from a direct comparison of experimental values. The reduction in emissions can also be predicted from a fumigant diffusion model (Yates, 2009) by increasing the injection depth from 46 cm to 61 cm. Conducting this analysis shows that the total 1,3-D emissions would be reduced by 21%, based on the predictions. This suggests that the benefit from deep injection should be approximately a 20% reduction in emissions, compared to standard fumigation; however, further research is needed to understand why the back-calculation methods yielded low values compared to the micrometeorological and predictive methods. A particular flux method produced relatively consistent maximum flux rates for the SI and DI experiments (Table 2). The difference between methods, however, was found to be greater. The ADM and CALPUFF methods produced Telone II flux rates between 25 and 33 μg m^{-2} s^{-1}, whereas the IHF, TPS, and ISCST3 methods were 12–18 μg m^{-2} s^{-1}, or approximately 50% lower rates. This has implications for risk assessment and for setting buffer zone sizes.

Additional research was conducted to further test these emission reduction strategies and for additional verification of the field results. Ashworth et al. (2009) conducted a laboratory study using soil from the field site. An experiment was conducted using 1.5 m stainless steel soil columns placed in a controlled temperature to simulate the temperature conditions observed at the field site. This study reported that the total emissions of 1,3-D after injection at 46 cm was 41%. For deep injection at 60 cm, total emissions of 1,3-D from replicated columns were found to be 26 ± 2% (unpublished data), which falls within the 20 ± 6% range. The laboratory value is also within 1% of the ADM and CALPUFF methods. Comparing total emissions after fumigant injection at 46 cm to deep injection (61 cm), led to a 36% reduction.

These results from the field experiments are consistent with two reports of the experimental uncertainty inherent with the methodology for calculating emission rates, where the accuracy was found to be from ±20–50%. Majewski (1997) reported that the accuracy for emissions of methyl bromide was approximately ±50% based on a regression analysis of the log-linear wind speed and concentrations profiles with respect to height, which should also apply to other fumigants that have log-linear concentration profiles. Wilson and Shum (1992) found that for appropriately large field sites with surface roughness lengths below 10 cm the IHF method would have experimental accuracy within approximately 20%. This analysis used a Lagrangian stochastic model and also provides guidelines that can be used in the design of field experiments.

Our experiments reveal considerable variability between the methodologies used for calculating the emission rate. However, it is difficult to state which method has the highest likelihood of being most accurate. To do this quantitatively would require an absolute reference for comparing each methodology. All the approaches used in this study require inherent simplifications and assumptions that can affect the calculated flux rates. The ADM method requires a well-developed surface layer for measuring gradients (concentration, wind speed, and temperature) and the evaluation of an empirical term for stable and unstable atmospheric conditions, which could introduce uncertainty. The TPS method does not require a large fetch, requires measurement of the air concentration and wind speed at a single height and uses a sensor height that is

relatively unaffected by atmospheric stability. This approach is based the trajectory simulation model (Wilson et al., 1981) to calculate the sensor height and a flux correction factor (ratio of horizontal to vertical flux), so uncertainty would be introduced whenever the simulated atmospheric conditions deviate from actual conditions. The IHF method has relatively few model assumptions (i.e., uniform source strength and known upwind fetch distance), but is dependent on the accuracy of the concentration-height profile at the measurement site. For complex, expensive, and large-scale field experiments, especially those involving multiple simultaneous experiments, it is often cost-prohibitive to collect highly detailed concentration-height measurements, which can introduce uncertainty.

The ISCST3 is a steady-state atmospheric dispersion model, so uncertainty would be introduced for variable source strengths or when wind conditions are variable during an hourly time step. CALPUFF is a non-steady-state Lagrangian puff model that tracks a fumigant in the atmosphere in a more natural manner, likely performing better than ISCST3, but the results depend on the gridding system employed and the representativeness of the meteorological data.

It is clear that further research is needed to better understand the accuracy and performance of these methods for calculating fumigant emissions.

Acknowledgment

The use of trade, firm, or corporation names in this research article is for the information and convenience of the reader. Such use does not constitute an official endorsement or approval by the United States Department of Agriculture or the Agricultural Research Service of any product or service to the exclusion of others that may be suitable. The authors are grateful to Q. Zhang and J. Jobes for their assistance in preparing and conducting this experiment. Part of the research described was supported by California Air Resources Board (agreement #05-351).

Appendix A. Supplementary data

Supplementary data related to this article can be found at http://dx.doi.org/10.1016/j.atmosenv.2016.04.042.

References

ARB (Air Resources Board-State of California), 1978. Air Pollution Emissions Associated with Pesticide Applications in Fresno County. Report ARB A7-047-30. Air Resources Board, Sacramento, CA, p. 310.

ARB (Air Resources Board-State of California), 1997a. Draft Emission Inventory Report-1995. Draft Report. Air Resources Board, Sacramento, CA, p. 38.

ARB (Air Resources Board-State of California), 1997b. Draft Emission Inventory Tables-1995. Draft Report. Air Resources Board, Sacramento, CA, p. 324.

Ashworth, D.J., Zheng, W., Yates, S.R., 2008. Determining breakthrough of the soil fumigant chloropicrin from 120 mg XAD-4 sorbent tubes. Atmos. Environ. 42, 5483–5488.

Ashworth, D.J., Ernst, F., Xuan, R., Yates, S.R., 2009. Laboratory assessment of emission reduction strategies for the agricultural fumigants 1,3-dichloropropene and chloropicrin. Environ. Sci. Technol. 43, 5073–5078.

Ashworth, D.J., Yates, S.R., van Wesenbeeck, I.J., Stanghellini, M., 2015. Effect of co-formulation of 1,3-dichloropropene and chloropicrin on evaporative emissions from soil. J. Agric. Food Chem. 63, 415–421.

Barry, T.A., Segawa, R., Wofford, P., Ganapathy, C., 1997. Off-site air monitoring following methyl bromide chamber and warehouse fumigations and evaluation of the Industrial Source Complex-Short Term 3 air dispersion model. In: Seiber, J., et al. (Eds.), Fumigants, ACS Symposium Series. American Chemical Society, Washington, DC, pp. 178–188, 1996. 652.

Brutsaert, W., 1982. Evaporation into the Atmosphere. Reidel, Dordrecht, 299 pp.

CDFA (California Department of Food and Agriculture), 1990. Use of Pesticide Suspended by CDFA. News Release No. 90–45, April 13, 1990, Sacramento, CA.

CDPR (California Department of Pesticides Regulation). California management plan: 1,3-dichloropropene. Department of Pesticide Regulation, Sacramento, CA. http://www.cdpr.ca.gov/docs/emon/methbrom/telone/mgmtplan.pdf.

CDPR (California Department of Pesticides Regulation), August 21, 2008. Memorandum Dated August 21, 2008 to Randy Segawa, Environmental Monitoring Branch, Memorandum. http://www.cdpr.ca.gov/docs/emon/pubs/ehapreps/analysis_memos/2071_segawa.pdf.

Denmead, O.T., Simpson, J.R., Freney, J.R., 1977. A direct field measurement of ammonia emission after injection of anhydrous ammonia. Soil Sci. Soc. Am. J. 41, 1001–1004.

Federal Register, 2000. Protection of Stratospheric Ozone: Incorporation of Clean Air Act Amendments for Restrictions in Class I, Group VI Controlled Substances, vol. 65, pp. 70795–70804.

Fleagle, R.G., Businger, J.A., 1980. An Introduction to Atmospheric Physics In: International Geophysics Series, second ed., vol. 25. Academic Press, New York. 432 pp.

Gan, J., Yates, S.R., Ernst, F.F., Jury, W.A., 2000. Degradation and volatilization of the fumigant chloropicrin after soil treatment. J. Environ. Qual. 29, 1391–1397.

Gao, S., Trout, T.J., 2006. Using surface water application to reduce 1,3-dichloropropene emission from soil fumigation. J. Environ. Qual. 35, 1040–1048.

Glotfelty, D.E., Taylor, A.W., Turner, B.C., Zoller, W.H., 1984. Volatilization of surface-applied pesticides from fallow soil. J. Agric. Food Chem. 32, 638–643.

Johnson, B., Barry, T., Wofford, P., 1999. Workbook for Gaussian Modeling Analysis of Air Concentration Measurements. California Environmental Protection Agency, Sacramento, CA.. Report EH99-03, September 1999 (Revised May 2010). 61 pp.

Jury, W.A., Spencer, W.F., Farmer, W.J., 1983. Behavior assessment model for trace organics in soil: 1. Model description. J. Environ. Qual. 12, 558–564.

Majewski, M.S., McChesney, M.M., Woodrow, J.E., Prueger, J.H., Seiber, J.N., 1995. Aerodynamic measurements of methyl bromide volatilization from tarped and nontarped fields. J. Environ. Qual. 24, 742–751.

Majewski, M.S., 1997. Error evaluation of methyl bromide aerodynamic flux measurements. In: Seiber, J.N., Knuteson, J.A., Woodrow, J.E., Wolfe, N.L., Yates, M.V., Yates, S.R. (Eds.), Fumigants: Environmental Fate, Exposure, and Analysis, ACS Symposium Series 652. American Chemical Society, Washington, DC, pp. 135–153.

McDonald, J.A., Gao, S., Qin, R., Thomas, J., 2008. Thiosulfate and manure amendment with water application and tarp on 1,3-dichloropropene emission reductions. Environ. Sci. Technol. 42, 398–402.

Meroney, R.N., 1992. Dispersion in non-flat obstructed terrain and advanced modeling techniques. Plant Oper. Prog. 11 (1), 6–11.

Merriman, J.C., Struger, J., Szawiola, R.S., 1991. Distribution of 1,3-dichloropropene and 1,2-dichloropropane in big creek watershed. Bull. Environ. Contam. Toxicol 47, 572–579.

Obreza, T.A., Onterman, E.O., 1991. Small-scale groundwater monitoring for 1,3-dichloropropene in southwest Florida. Soil Crop Sci. Soc. Fla. Proc. 50, 94–98.

Parmele, L.H., Lemon, E.R., Taylor, A.W., 1972. Micrometeorological measurement of pesticide vapor flux from bare soil and corn under field conditions. Water Air Soil Pollut. 1, 433–451.

Pruitt, W.O., Morgan, D.L., Lourence, F.J., 1973. Momentum and mass transfers in the surface boundary layer. Q. J. R. Meteorol. Soc. 99, 370–386.

Reichman, R., Rolston, D.E., Yates, S.R., Skaggs, T.H., 2011. Diurnal variation of diazinon volatilization: soil moisture effects. Environ. Sci. Technol. 45, 2144–2149.

Reichman, R., Yates, S.R., Skaggs, T.H., Rolston, 2013a. D.E. Effects of soil moisture on the diurnal pattern of pesticide emission: numerical simulation and sensitivity analysis. Atmos. Environ. 66, 41–51.

Reichman, R., Yates, S.R., Skaggs, T.H., Rolston, D.E., 2013b. Effects of soil moisture on the diurnal pattern of pesticide emission: comparison of simulations with field measurements. Atmos. Environ. 66, 52–62.

Rosenberg, N.J., Blad, B.L., Verma, S.B., 1983. Microclimate, the Biological Environment. John Wiley & Sons, New York, 495 pp.

Ross, L.J., Johnson, B., Kim, K.D., Hsu, J., 1996. Prediction of methyl bromide flux from area sources using the ISCST3 model. J. Environ. Qual. 25, 885–891.

Schneider, R.C., Green, R.E., Wolt, J.D., Loh, R.K.H., Schmitt, D.P., Sipes, B.S., 1995. 1,3-Dichloro-propene distribution in soil when applied by drip irrigation or injection in pineapple culture. Pesti. Sci. 43, 97–105.

Scire, J.S., Strimaitis, D.G., Yamartino, R.J., 2000. User's Guide for the CALPUFF Dispersion Model. Earth Tech, Inc., Concord, MA, 521 pp.

Spencer, W.F., Cliath, M.M., 1973. Pesticide volatilization as related to water loss from soil. J. Environ. Qual. 2, 284–289.

Spencer, W.F., Cliath, M.M., Farmer, W.J., 1969. Vapor density of soil-applied dieldrin as related to soil-water content, temperature, and dieldrin concentration. Soil Sci. Soc. Am. Proc. 33, 509–511.

UNEP (United Nations Environment Programme), 1992. Methyl Bromide: its Atmospheric Science, Technology, and Economics. United Nations, Ozone Secretariat, P.O. Box 30552, Nairobi, 54 pp.

UNEP (United Nations Environment Programme), 1995. UNEP 1994 Report of the Methyl Bromide Technical Options Committee. United Nations, Ozone Secretariat, P.O. Box 30552, Nairobi.

Wang, D., Yates, S.R., Ernst, F.F., Gan, J., Jury, W.A., 1997. Reducing methyl bromide emission with a high barrier plastic film and reduced dosage. Environ. Sci. Technol. 31, 3686–3691.

Wilson, J.D., Shum, W.K.N., 1992. A re-examination of the integrated horizontal flux method for estimating volatilisation from circular plots. Agric. and. For. Meteor 57, 281–295.

Wilson, J.D., Thurtell, G.W., Kidd, G.E., 1981. Numerical simulation of particle trajectories in inhomogeneous turbulence, I: systems with constant turbulent

velocity scale. Bound. Layer. Meteor. 21, 295–313.
Wilson, J.D., Thurtell, G.W., Kidd, G.E., Beauchamp, E., 1982. Estimation of the rate of gaseous mass transfer from a surface source plot to the atmosphere. Atmos. Environ. 16, 1861–1867.
Yagi, K., Williams, J., Wang, N.Y., Cicerone, R.J., 1995. Atmospheric methyl bromide (CH3Br) from agricultural soil fumigations. Science 267, 1979–1981.
Yates, S.R., Ernst, F.F., Gan, J., Gao, F., Yates, M.V., 1996. Methyl bromide emissions from a covered field. II. Volatilization. J. Environ. Qual. 25, 192–202.
Yates, S.R., Gan, J., Wang, D., Ernst, F.F., 1997. Methyl bromide emissions from agricultural fields. Bare-soil, deep injection. Environ. Sci. Technol. 31, 1136–1143.
Yates, S.R., Knuteson, J., Ernst, F.F., Zheng, W., Wang, Q., 2008. The effect of sequential surface irrigations on field-scale emissions of 1,3-dichloropropene. Environ. Sci. Technol. 42, 8753–8758.
Yates, S.R., Knuteson, J., Zheng, W., Wang, Q., 2011. Effect of organic material on field-scale emissions of 1,3-dichloropropene. J. Environ. Qual. 40, 1470–1479. http://dx.doi.org/10.2134/jeq2010.0206.
Yates, S.R., Ashworth, D.J., Zheng, W., Zhang, Q., Knuteson, J., Van Wessenbeeck, I., 2015. Emissions of 1,3-dichloropropene and chloropicrin after soil fumigation under field conditions. J. Agric. Food Chem. 63, 5354–5363. http://dx.doi.org/10.1021/acs.jafc.5b01309.
Yates, S.R., 2009. Analytical solution describing pesticide volatilization from soil affected by a change in surface condition. J. Environ. Qual. 38, 259–267.
Yon, D.A., Morrison, G.A., McGibbon, A.S., 1991. The dissipation of 1,3-dichloropropene in ditch sediment and associated aerobic ditch water. Pest. Sci. 32, 147–159.